

# Experimental Characterisation of TRIP Effects of 31CrMoV9 for Hot Forming

Peddinghaus Simon<sup>1,a\*</sup>, Mohnfeld Norman<sup>1,b</sup>, Uhe Johanna<sup>1,c</sup>,  
Behrens Bernd-Arno<sup>1,d</sup>

<sup>1</sup>Leibniz University Hannover, Institute of Forming Technology and Machines, An der Universität 2,  
30823 Garbsen, Germany

<sup>a\*</sup>s.peddinghaus@ifum.uni-hannover.de, <sup>b</sup>mohnfeld@ifum.uni-hannover.de,  
<sup>c</sup>uhe@ifum.uni-hannover.de, <sup>d</sup>behrens@ifum.uni-hannover.de

\*corresponding author

**Keywords:** hot forming, TRIP, material characterisation.

**Abstract.** During the hot bulk forming of long parts, inhomogeneous distributions of deformations and temperatures occur. The gradients of these distributions lead to complex, overlaying residual stresses, which can cause critical geometric deviations and mechanical failures. Common finite element (FE)-simulations for designing a process are in principle capable to predict the thermal, mechanical and metallurgical effects, but require extended material models. Thereby, the total strain increment can be described through the partial strain components of the elastic, plastic, thermal transformation related and transformation plasticity strain. To allow the numerical prediction of the distortion of long hot formed parts, an experimental characterisation of the transformation-induced plasticity (TRIP) and backflow effects is presented for the steel 31CrMoV9. Time temperature transformation (TTT) and continuous cooling transformation (CCT) diagrams are determined with JMatPro and verified by means of microstructure analysis and hardness measurements. Based on these diagrams, the transformation plasticity is investigated through dilatometric tests whereby tensile and compressive loads are applied during the phase transformation. The martensite phase transformation showed the highest amounts of TRIP of 1.55 % strain under tensile loads and 1.32 % strain for compressive loads, whilst the bainite transformation exhibited lower strains of 0.7 % in the tensile load case and 0.74 % in the compression load case, but a high tensile backflow strain of 0.56 %. For pearlite the beginning of the phase transformation was delayed and its duration extended due to the induced loads.

## Introduction

To manufacture high-performance parts with complex geometries through hot bulk forming, high forces are applied at elevated temperatures to achieve high degrees of plastic deformation [1]. Thereby numerous varying effects occur within the workpiece itself, like phase transformations, or at the interface between the workpiece and the die, such as heat transfer and friction. For steel, during thermo-mechanical processing multiple interrelated phenomena occur. Their interactions can cause defects as for example critical distortions [2]. In hot bulk forming processes, these phenomena develop unsteady in terms of time and location. As the distribution of the aforementioned effects is particularly inhomogeneous in geometrically complex or long parts with uneven mass distributions, they are vulnerable to distortion, which can lead to scrap production and is costly especially for big parts [3]. FE simulations allow to predict and prevent such critical phenomena through an adjusted process design. In numerical simulations, the additive strain composition method as shown in equation 1, can be applied, whereby the five strains: elastic ( $\varepsilon_{ij}^{el}$ ), plastic ( $\varepsilon_{ij}^{pl}$ ), thermal ( $\varepsilon_{ij}^{th}$ ), transformation related (tr) and transformation plastic (tp), are considered separately. The partial strains are determined separately from the current thermal, metallurgical and mechanical conditions, added up and then applied as total strain increment [4].

$$d\varepsilon_{ij}^{total} = d\varepsilon_{ij}^{el} + d\varepsilon_{ij}^{pl} + d\varepsilon_{ij}^{th} + d\varepsilon_{ij}^{tr} + d\varepsilon_{ij}^{tp} \quad (1)$$

The individual strains require extended material models determined either through thermodynamical computation (e.g. through JMatPro) or an experimental characterisation. The elastic and plastic strains can be derived from well-known characterisation tests such as compression or tensile tests. The thermal and transformation related strains are caused by volumetric changes, either of the heat expansion or phase transformations, such as from austenite to ferrite, pearlite or martensite and can be determined using conventional dilatometric tests. When such phase transformations are overlayed by other mechanically or thermically induced stresses, the so-called transformation-induced plasticity leads to transformation plastic strains and isotropic transformation stresses in dependence of the applied mechanical loads. When the overlaying stresses are released during the transformation, a part of the TRIP strain can form back due to the so-called backflow effect [5]. This effect is particularly relevant for hot bulk forming processes, as they show inhomogeneously distributed and changing stresses [6].

The experimental characterisation of the transformation plastic strain however, presents a challenging task. On the one hand, in contrast to the other partial strains, no widely established norms or standards exist regarding the experimental method or the equipment. On the other hand, the approaches of current research require extensive prior knowledge of the time and temperature dependent phase transformations. For this, continuous cooling transformation (CCT) and time temperature transformation (TTT) diagrams have to be determined either numerically or experimentally.

Additionally, in terms of modelling, for the elastic, plastic, thermal and the transformation related strains, established models such as the flow curve approach of Hensel Spittel [7], are available and corresponding material parameters for a wide range of materials can be found either in databases or the results of numerous research work such as [8] or [9]. However, for the transformation plastic strain, there is neither a standardised experimental approach, nor sufficient corresponding material data available through data bases or in literature.

In the state of the art, to experimentally characterise the transformation induced plasticity under the thermomechanical conditions of hot forging, TTT- diagrams are used to identify cooling routes to achieve full transformations of the individual phases. These transformation processes are then overlayed with mechanical stresses through compression or tension of the specimen, as demonstrated for example by Lakhdar et al. [10] and Holzweissig et al. [11]. The backflow effect is investigated through additional tests, where the applied stresses are removed during the transformation [12]. The corresponding TRIP and backflow coefficients can be determined from the experimental data either by means of an analytical approach as in [13] or numerically iteratively through the comparison of experimental and numerical results [3]. For this, for example Suhr et al. in [14] as well as Behrens et al. in [3] implemented the TRIP equations into commercial FE software and validated their approaches by recreating the strain behaviour of the experimental tests.

For hot forging processes of a 42CrMo4 steel, Behrens showed that the complete incremental strain can be modelled in detail based on an extensive material characterisation which allowed to predict the distortion of a hot bulk formed workpiece [6]. However, this approach is not applied widely, because it requires very detailed material data, which requires specialised testing equipment and a large amount of testing and is not available in the literature. Although the fundamental phase transformations to pearlite, bainite and martensite occur for most steels, the time and temperature dependent transformation behaviour strongly varies in dependence of the alloying elements [15]. Therefore, findings and models with regards to the TRIP and backflow behaviour are not directly transferable and require separate characterisations.

The steel 31CrMoV9 is usually applied for manufacturing heavily loaded components through hot forging as a high strength can be reached after heat treatment. Additionally, it can be nitrided deeply to achieve a higher wear resistance [16]. As severe residual stresses are induced during the nitration process, a detailed knowledge of the occurring stresses and strains is essential for an optimised development of products made of 31CrMoV9 [17]. However, little to no experimental data can be found about the transformation-induced plasticity and the backflow effects of 31CrMoV9.

Therefore, this paper presents an investigation of the TRIP behaviour of the steel alloy 31CrMoV9 in a quenched and tempered state. The results shall also allow to derive TRIP coefficients for following numerical simulations. First, a material dataset is created numerically using JMatPro as a basis to define heating-cooling routes for the phase transformation to pearlite, bainite and martensite. After the cooling routes are verified through stress free tests and microstructure analysis with hardness measurements, the experimental setup of Behrens et al. is applied to investigate the TRIP and backflow effects for varying loads [12].

## Material and Methods

The experimental determination of TTT and CCT-diagrams requires a great amount of costly and time-consuming tests whilst the resulting diagrams are only applicable for specific process conditions. To reduce the test effort, the TTT and CCT-diagrams were calculated with the material simulation software JMatPro based on the application for hot forming and on the chemical composition determined through optical emission spectrometry, as shown in table 1.

**Table 1.** Chemical composition of the investigated steel 31CrMoV9 (in wt%).

Steel grade	C	Si	Mn	P	S	Cu	Cr	Ni	Al	Mo	V	Ti	Nb
31CrMoV9	0.329	0.272	0.632	0.009	0.002	0.127	2.48	0.123	0.025	0.19	0.143	0.012	0.004

The TTT and CCT-diagrams were calculated for an austenisation at 1,200 °C to recreate the conditions of hot bulk forming [1] as illustrated in Fig. 1. The CCT-diagram in Fig 1 a) shows that, for example a pearlite transformation can be expected when the temperature has not dropped from 1,200 °C to under approximately 530 °C within roughly 500 s after the forming process. As after hot forming, especially of large parts, a cooling process can take considerable longer and has an inhomogeneous temperature distribution, each of the three phase transformations is investigated [1].

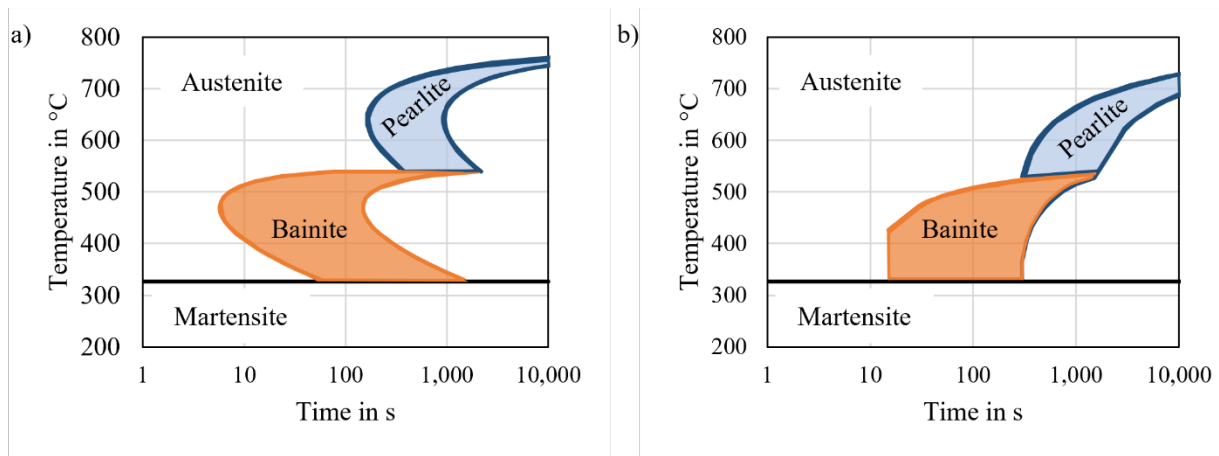


**Fig. 1.** a) TTT and b) CCT-diagrams of 31CrMoV9 determined using JMatPro with the transformation areas of Bainite (B), Pearlite (P) and Martensite (M) from Austenite(A).

In addition to the TTT and CCT-diagrams, flow curves were determined with JMatPro. As illustrated in Fig. 2, the applied axial loads 100 MPa of Behrens et al. do not exceed the flow stresses of the base material at 450 °C but at 650 °C until a plastic deformation of 0.02 [12]. As the base material shows overall lower flow stresses than the individual phases at the corresponding temperatures, it can be excluded, that an unwanted plastic deformation occurs after the phase transformation which would overlay the TRIP effects.

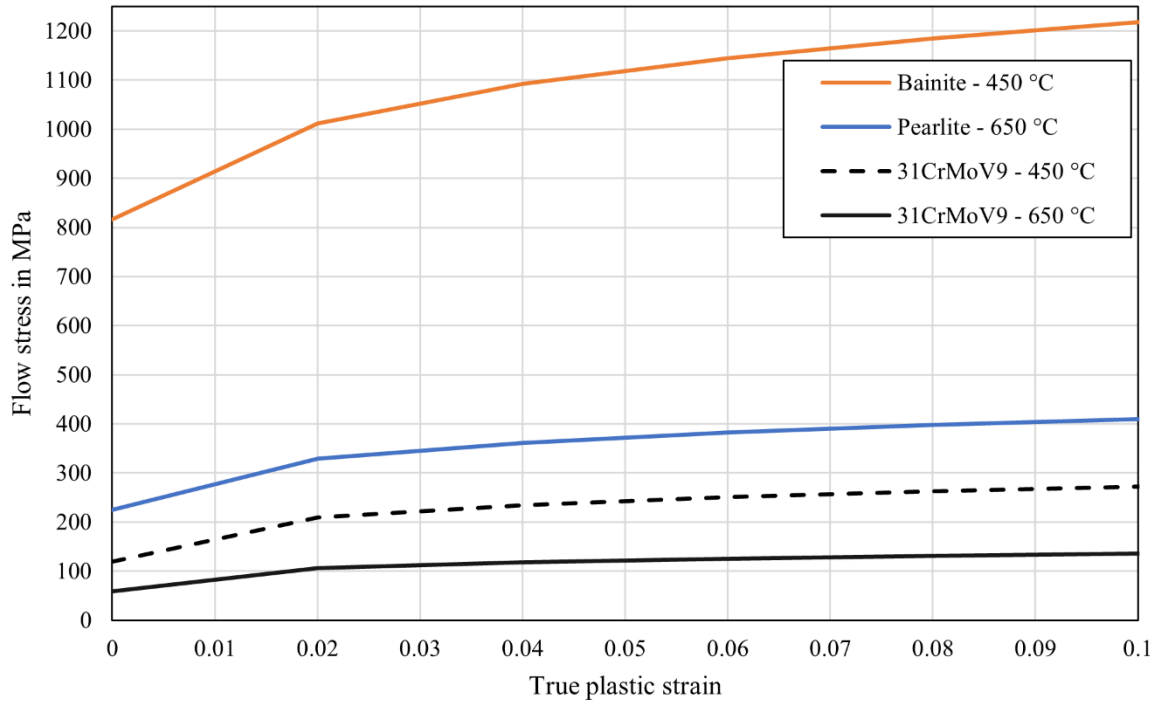


**Fig. 2.** Flow curves of 31CrMoV9 determined with JMATPro for the base material as well as for of bainite and pearlite.

The experimental investigation of the TRIP and backflow effects, was carried out with a quenching and deformation dilatometer DIL 805 A/D+T (TA instruments). The specimens were taken from billets for a hot forming process, which were hot rolled and then quenched and tempered. As shown in Fig. 3, the specimen geometry has a tapered testing area in the middle with a diameter of 5 mm and a length of 10 mm. The specimen is clamped by threads at each end to allow the application of tensile as well as compressive loads through a hydraulic cylinder at the moveable specimen holder. Changes of the length are measured using quartz pushing rods at the edges of the tapered testing area. The temperature is controlled with a thermocouple type K, which is welded on the surface at the middle of the specimen.

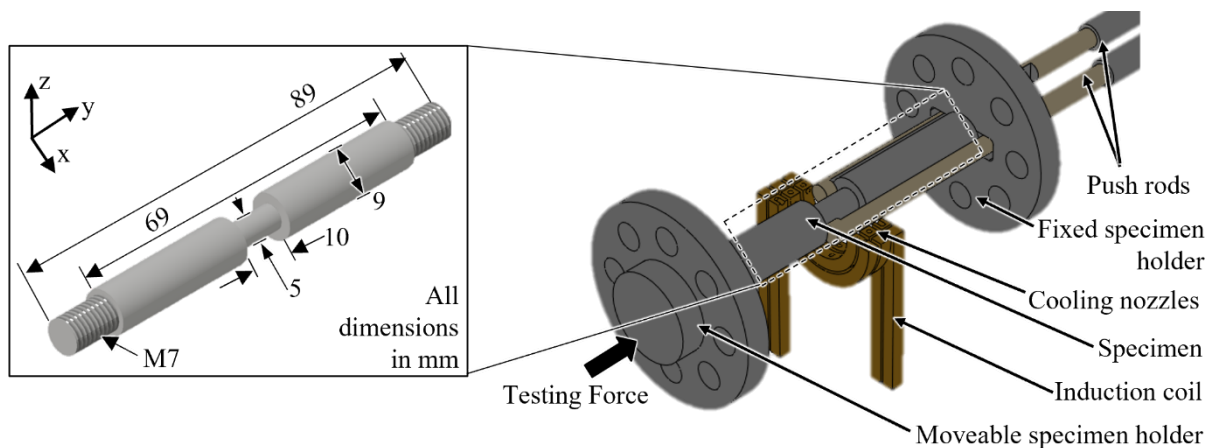


**Fig. 3.** Schematic experimental test setup with the detailed geometry of the test specimen.

During the experiment, the specimen is heated inductively in a vacuum atmosphere to an austenisation temperature of 1,200 °C with a rate of 10 K/s, held for 120 s to homogenise the temperature distribution and then cooled down at controlled rates with helium gas from nozzles in the induction coil. As the cooling of forging.

Based on the TTT-diagrams, individual cooling routes are defined for the diffusion-based phase transformations to pearlite, bainite and the diffusionless transformation to martensite as shown in Fig. 4. For the phase transformation to pearlite, a temperature of 650 °C is held for 1,700 s. For the bainite transformation, a temperature of 450 °C with a holding time of 250 s is chosen. In order to minimise other transformation processes, the highest possible stable cooling rate of the machine of 50 K/s is chosen for the martensite transformation and for the cooling from the austenitisation to the individual holding temperatures of the other phase transformations.

To characterise the TRIP effect, each of the three phase transformations was superimposed with mechanical stresses as illustrated in Fig. 4. As in the experiments of [3] and [12], axial loads of 1,964 N, corresponding to 100 MPa, are applied throughout the complete transformations as compression or tension. As this exceeds the flow stress at 650 °C as shown in Fig. 2, for the pearlite transformation, additional tests were carried out with 982 N, corresponding to 50 MPa.

To avoid plastic deformation before the martensite transformation, the loads were induced once a temperature of 450 °C was reached. In additional tests to investigate the backflow effects, the loads are removed after approximately the half of the time of the transformation based on the TTT-diagrams from JMatPro. For each cooling route and load case, the tests were repeated three times.

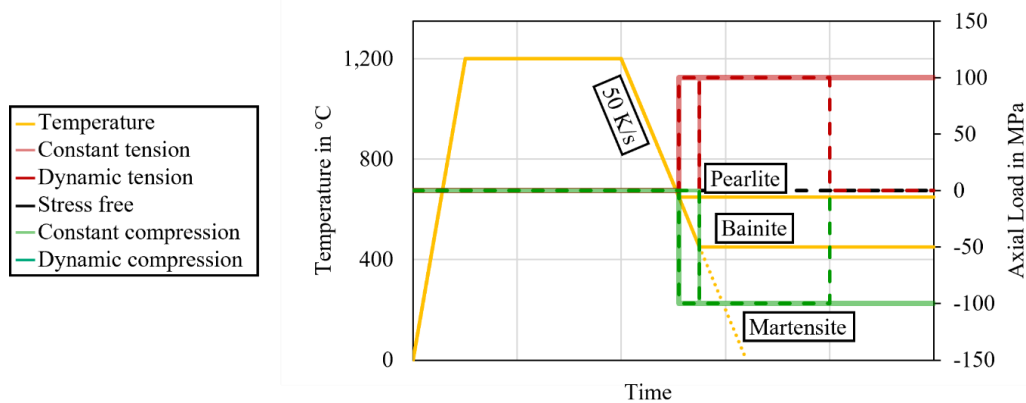


**Fig. 4.** Test procedure with investigated temperatures and axial loads.

To verify the cooling route for each of the phase transformation, the microstructure was characterised. Therefore, specimens of the stress free tests were cut from the middle of the parts, embedded, grinded, and polished to 0.5  $\mu\text{m}$  and then etched with  $\text{HNO}_3$ . Additionally, for each cooling route, hardness measurements (HV0.5) were carried out.

## Results and Discussion

The microstructures resulting from the cooling routes for the different phase transformations are compared in Fig. 5. In the microstructure of the specimens which were held at 650 °C in Fig. 5 a), a pure and homogenic pearlite structure can be observed, with a hardness of 221 HV0.5 to 274 HV0.5. The microstructure of the cooling route at 450 °C mostly consists of bainite, which is recognisable as bright blue structure with an average hardness of 466 HV0.5. However, as shown in Fig. 5 c), small portions of a different brown-colored structure can be noticed. The cooling route directly to room temperature with a cooling rate of 50 K/s results in a fine martensitic structure with an average hardness of 610 HV0.5 as shown in Fig. 5 c). In the microstructures of the cooling route for bainite and for martensite, bright stripes in the longitudinal direction of the specimen can be seen. As the hardness is the highest in these stripes with approximately 700 HV0.5, a possible explanation for these could be, that the stripes consist of carbide precipitations resulting from the prior hot rolling of the specimens. The microstructure analysis with the hardness measurements demonstrates that the chosen cooling routes lead to the targeted phase transformation and therefore can be considered suitable for the following experimental investigations, although the influence of the presumed carbides and also the uncertainty in the bainite has to be taken into consideration for the discussion of the experimental results.

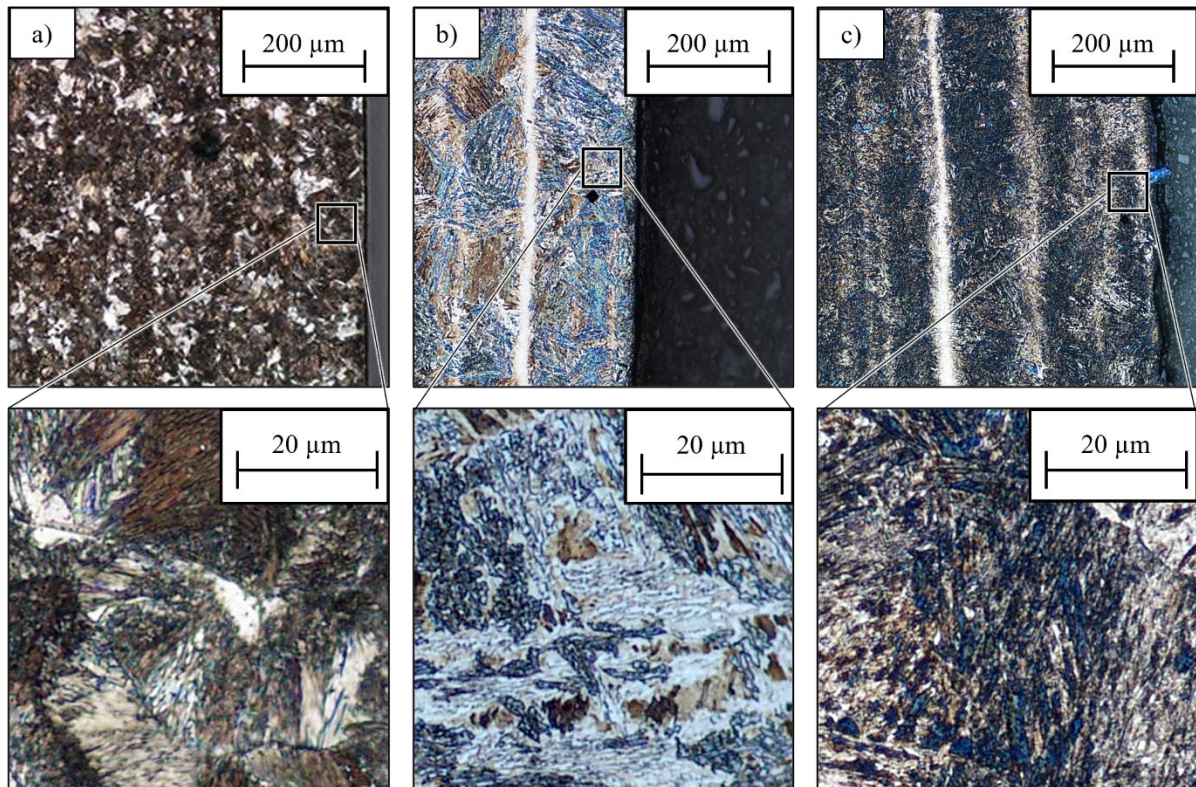


**Fig. 5.** Microstructure analysis in the testing area of the specimens of the stress free tests: a) pearlite transformation, b) bainite transformation and c) martensite transformation.

The TRIP and the backflow strains are determined similar to work of [12] with the middle curve of the three repetitions of each parameter configuration. The range between the minimum and maximum curve of each investigated parameter configuration are visualised in the analysis diagrams as surfaces around the corresponding curve to emphasise the deviations between the repetitions.

Thereby, the TRIP strain is determined from the difference of the length change of the constantly loaded curve and the stress free curve at the end of the transformation. For the backflow strain, the difference between the constantly and the dynamically loaded curves at the end of the transformation is calculated.

During the pearlite transformation, multiple effects can be observed as illustrated in Fig. 6. After the holding temperature of 650 °C is reached, the stress free curve shows a constant value for the length change, until at approximately 900 s an increase can be noted. After this increase the curve converges towards a constant level at a value of 0.33 %. This length change at a constant temperature is caused by the phase transformation from austenite to pearlite with the corresponding volumetric change as for example outlined in [18]. This transformation occurs as predicted in the TTT-diagrams, which is in agreement to the findings of the microstructure analysis that the chosen cooling route is suitable for the investigation of the TRIP and backflow effects.

For both load cases, the length of the specimen abruptly changes by approximately 0.75 % once the axial loads are applied. After the abrupt increase, linear changes of the curves can be observed. For the tensile load case the length increases and for the compressive load it decreases. The abrupt length changes after the loading followed by the steady change indicate that the axial loads exceeded the flow stress and led to a plastic deformation in addition to the TRIP effects as the flow curves in Fig. 2 indicated. Also, for the application of high axial loads at elevated temperatures for relatively long times, the influence of creep cannot be excluded. Due to the stresses slightly under the level of the flow stress, which are held after the initial plastic deformation, the steady length changes could be overlaid by creep in addition to TRIP effects.

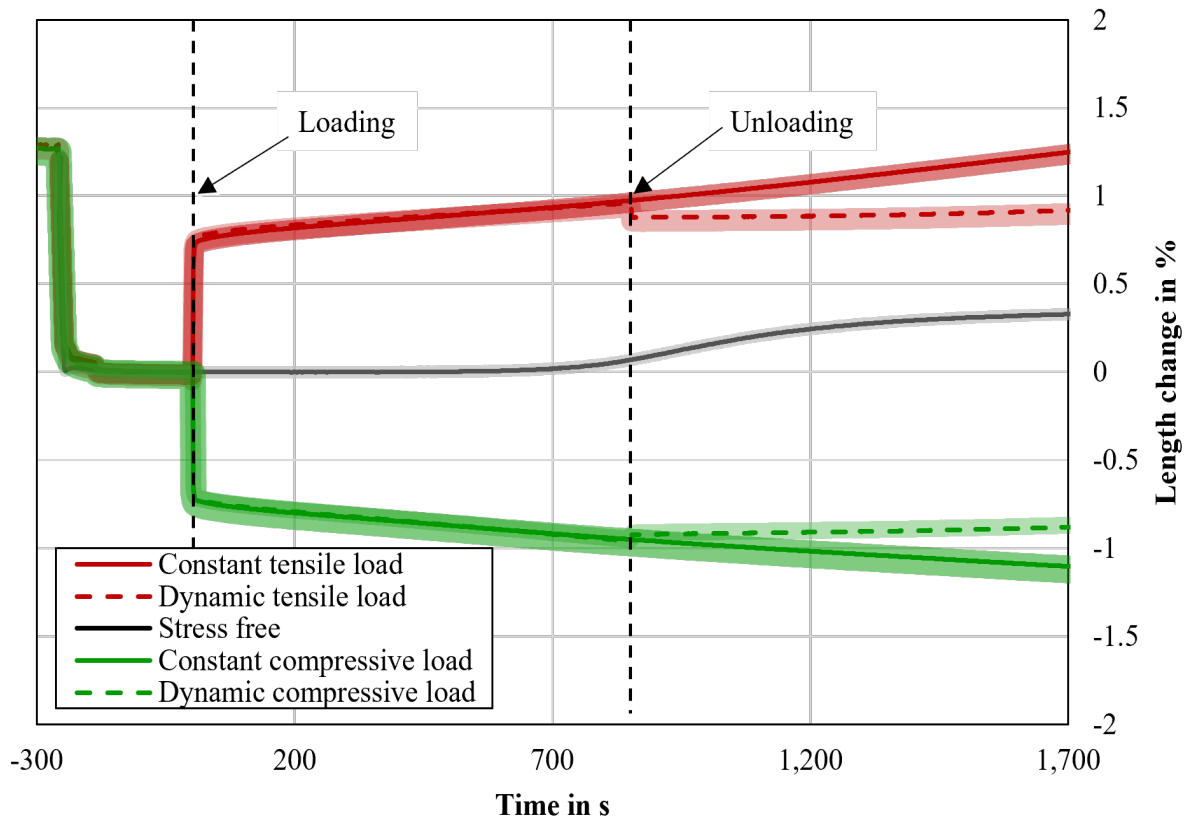


**Fig. 6.** Experimental results of the pearlite transformation at a holding temperature of 650 °C for varying load cases with 100 Mpa.

In contrast to the tests with axial loads of 100 MPa, the pearlite phase transformations superimposed with 50 MPa show a less abrupt increase after load is applied whilst also having overall lower amounts of length changes. As compared in Fig. 7, the loaded curves only show a slight length change after the initial increase due to the load application. The tensile tests exhibit higher length changes than the compression tests. After the full test time of 1700 s however, the absolute length changes for both load cases, of 0.2 % for compression and 0.35 % for tension, are lower or very close to the corresponding amount of the stress free case. As the curves of both load cases also show an increase or decrease after 1700 s in contrast to the stress free curve, it is questionable if a complete phase transformation was observed. The dynamic tensile load case shows an abrupt decrease once the load is removed and decreases almost completely back to the initial level before the loads were applied, which means that to that point none or only reversible TRIP effects have occurred. On the one hand this proves that the applied loads have not exceeded the flow stress as for 100 MPa and on the other hand it suggests that within the 1700 s only a minor phase transformation has occurred. To investigate this more in detail, an additional test series was carried out, whereby the specimens were held under a constant tensile load at the transformation temperature of 650 C for a total time of 4,100 s and thereby 2,400 s longer than before. In the longer tests, as displayed in Fig. 7, it can be seen that the length change shows a longer increase and exceeds the values of the stress free curve. Thereby, even though the gradient decreases, it does not completely flatten before the end of the test. As the effects of creep are expected to be negligibly low for 50 MPa and the investigated holding times, the ongoing length change indicates that the phase transformation is not completed after 4,100 s.

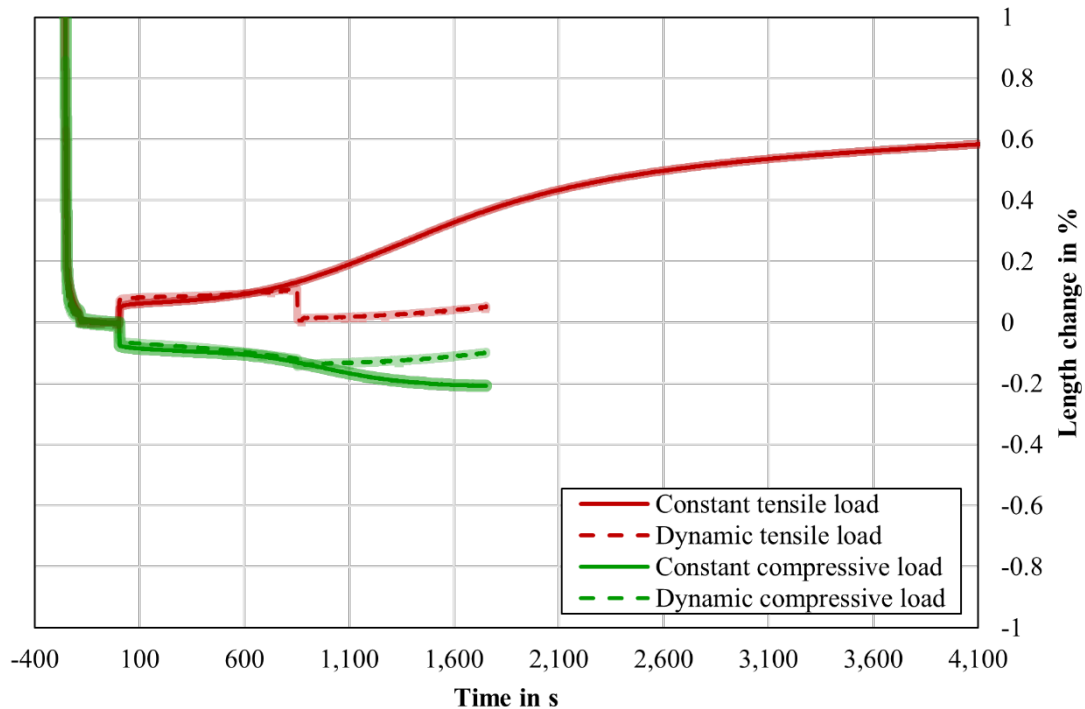


**Fig. 7.** Experimental results of the pearlite transformation at a holding temperature of 650 °Cs for varying load cases with 50 Mpa.

The considerable differences of the curves under the axial loads of 50 MPa in comparison to the stress free case lead to the conclusion that the beginning time and the duration of the phase transformation has been strongly shifted and flattened. The phase transformation was not completed after a testing time of 4,100 s, whilst still showing comparatively low length changes. As this was observed for 50 MPa, it is unlikely that for 100 MPa a phase transformation occurred within the test time. As the flow stress was exceeded, it is more likely that the length changes, even after the initial plastic deformation, were caused through creep than TRIP. Therefore, the tests with 100 MPa are not suitable for the investigation of the TRIP and backflow effects of pearlite, as the time and temperature dependent transformation behaviour changes in dependence of deformation and a clear separation of plastic deformation, creep and TRIP is not possible. For a more detailed investigation of the TRIP and backflow effects of the pearlite phase transformation of 31CrMoV9, additional tests with a longer holding time have to be considered. Thereby it is expected that due to the duration of the phase transformation a considerably high experimental and numerical effort is required. Also, for longer holding times at the elevated temperatures of the pearlite transformation, an increased influence of creep is expected, which would require a separate characterisation through additional tests.

However, in comparison to the cooling routes of common hot forming processes, particularly of long parts, the time until the transformation begins and the duration are relatively long [1]. While the time period observed for the stress free pearlite transformation could still be relevant for the cooling of large forged parts, it is most likely that when stresses are induced the phase transformation is strongly delayed as well as slowed down and thereby reduced to an insignificant amount. Hence, it can be concluded that the pearlite transformation and the corresponding transformation induced plasticity only have a marginal effect on the resulting part geometry and therefore can be neglected for an efficient process design of products made of 31CrMoV9.

In comparison to the phase transformations of the pearlite and the martensite, the bainite transformation does not show a substantial characteristic length change to identify the time interval of the phase transformation, as depicted in Fig. 8. The stress free curve only shows a slight and steady decline of the length change. However, as the decline can be observed for a constant temperature, it can be concluded that a phase transformation occurs with the chosen cooling route. On the one hand, according to the TTT-diagrams, the transformation starts immediately once the holding temperature

is reached, which makes it difficult to distinguish the beginning of the transformation. On the other hand, the differences in volume between austenite and bainite are relatively low compared to the other phase transformations, as illustrated in [18]. Between the different load cases, clear differences can be noted. Under compressive load, the curve of the length change shows a stronger decrease after the load is applied. During the ongoing transformation, the slope of the curve is close to the stress free curve whilst showing a slightly stronger decrease indicating TRIP strain effects. The load-dependent behaviour of the curves is in agreement with the findings of [19]. In contrast to the other two load cases, the curve of the tensile load increases steadily after the load is applied. As the curves of both load cases do not show an abrupt increase after the loads are applied, it can be concluded, that the flow stress was not exceeded in agreement to Fig. 2 and plastic deformation did not occur.

The curves of both constant load cases do not show a change of their gradient, which would indicate the end of the transformation. As the holding times and temperatures of the bainite transformation are comparably low, the influence of creep is assumed as negligible. In combination with the microstructure analysis in Fig. 5, which did not show a complete bainite structure, this leads to the conclusion, that the transformation might not have been completed within the test. Therefore, the strains can only be evaluated for a partial phase transformation. After 250 s an absolute TRIP strain of 0.7 %, with a backflow of 0.15 % for the compressed load whilst for the tensile loading a TRIP strain of 0.74 %, with a backflow of 0.56 % strain can be determined. The ratio of the backflow to the TRIP strain for the tensile load case is noticeably high in comparison to the compressive load and also to the corresponding ratios of 0.45 % and 0,6 % to 1.55 % and 1.32 % for the martensite phase transformation. This could be related to the presumed incomplete transformation. To analyse the complete phase transformation of the bainite, tests with a longer holding time are required. Also, the presumed incomplete transformation is in contradiction to the numerically determined TTT-diagrams which indicate that the bainite transformation is completed within the testing time. Taking the uncertainty observed in the microstructure into consideration, this emphasizes that additional experimental tests are required to determine the real time and temperature dependent transformation behaviour of the investigated material. However, with appropriate TTT-diagrams, the recorded curves could be sufficient to derive approximate TRIP coefficients as presented in [20], as the inverse numerical fitting approach can also be applied to incomplete transformations.

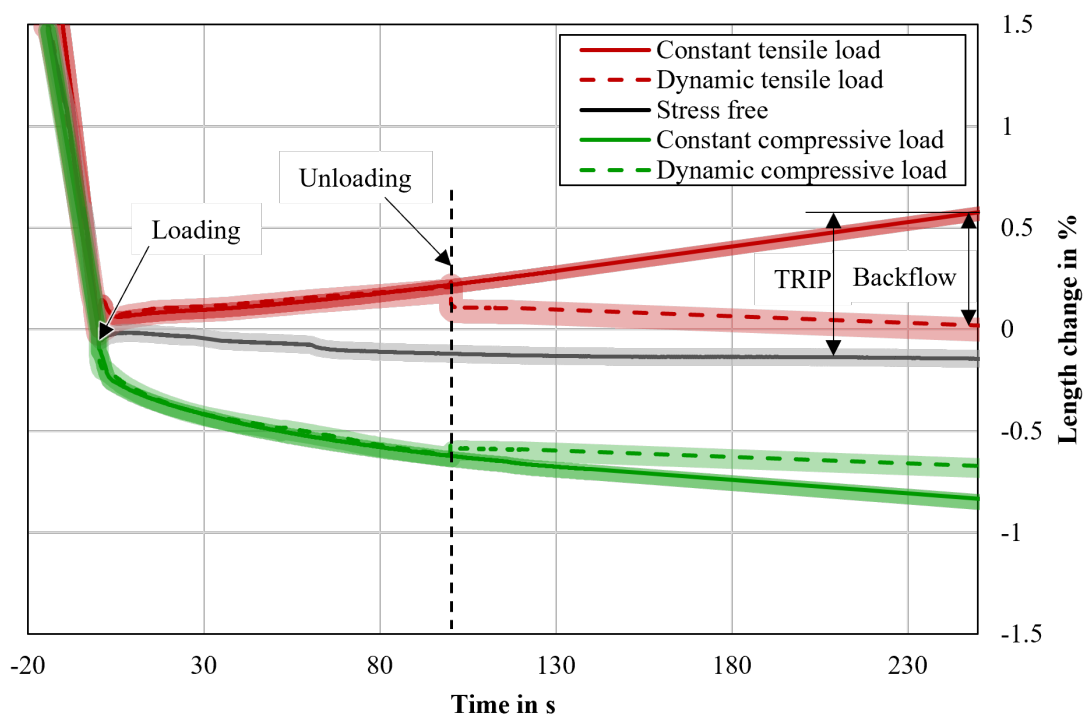


**Fig. 8.** Experimental results of the bainite transformation at a holding temperature of 450 °C for varying load cases.

As martensite is formed by a diffusionless transformation, the phase transformation does not take place at a constant temperature, but a constant cooling rate of 50 K/s. Therefore, all of the recorded curves show a constant length change with a linear trend and a turning point at approximately 280 °C as illustrated in Fig 9. At this point, the length change first increases strongly and then converges to the same gradient as before. This slope change indicates the phase transformation from the cubic face-centered austenite to tetragonal body-centered martensite, which leads to an increase in volume. Without applied forces, the transformation leads to a shift in the curve of 0.7 % length change. In comparison to the stress free curve during the phase transformation, the curve of the tensile load shows a stronger increase of the length change whilst the compressive loaded test shows a lower increase. At the end of the phase transformation, a TRIP effect of 1.55 % strain for the tensile loaded and 1.32 % strain for the compressive loaded can be determined. From the comparison of the constantly and dynamically loaded curves corresponding backflow strains of approximately 0.45 % length change for the tensile loaded test and 0.6 % length change for the compressive load can be determined. The TRIP strains of the martensite transformation show the tendency of higher TRIP strains for tensile loads, which is in agreement with the results of [12].

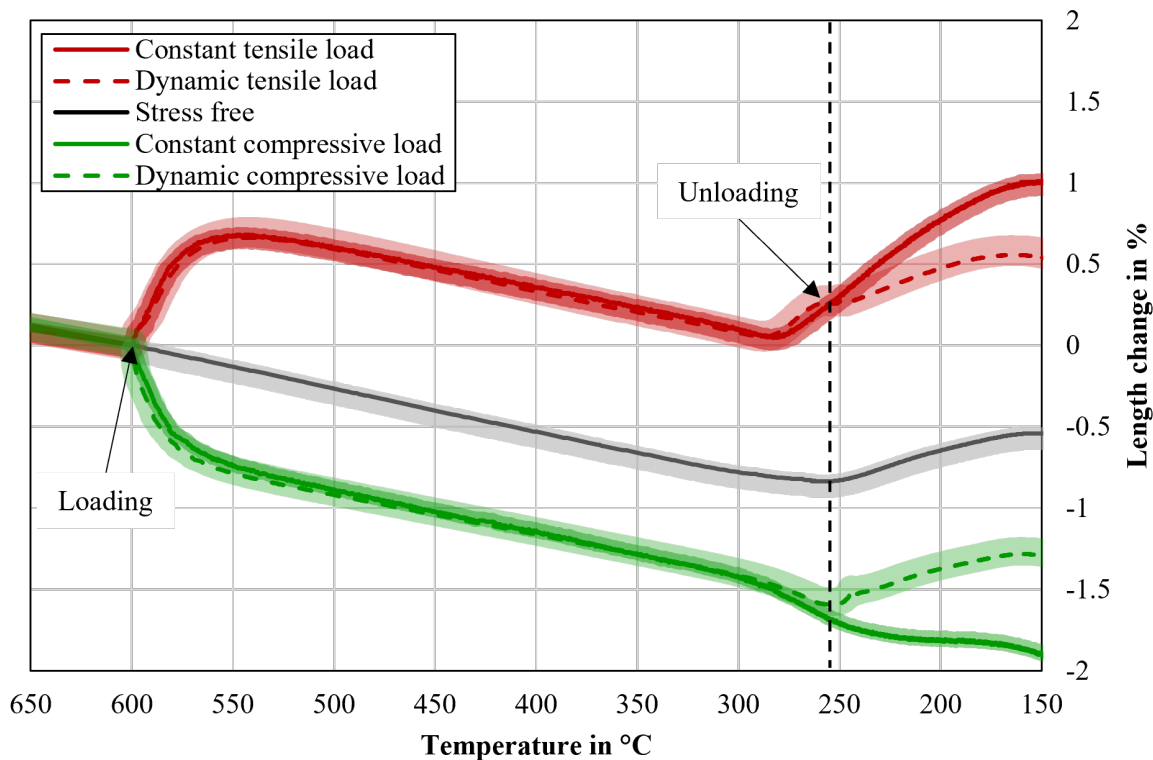


**Fig. 9.** Experimental results of the martensitic transformation with a cooling rate of 50 K/s for varying load cases.

As hot bulk formed parts usually cool down without any immediate heat treatment which includes a holding of the temperature, the predominant phase transformations are expected to be from austenite to bainite and martensite. Of the investigated transformations, the martensite phase transformation shows the most TRIP strains and also the most volumetric change when no stress is applied, which is in agreement with the results of [18]. This leads to the effect, that in comparison to the other transformations, on the one hand during the transformation to martensite more residual stresses form due to the volumetric changes and on the other hand such present stresses also lead to more TRIP strain. Therefore, it can be concluded that the martensitic transformation presents the most critical transformation to consider in numerical simulations of hot forming processes of 31CrMoV9.

## Summary and Outlook

In this paper, the TRIP and backflow effects of the steel 31CrMoV9 were investigated. Based on numerically calculated TTT-diagrams, suitable cooling routes were defined. The cooling routes were verified through microstructure analysis and hardness measurements. The TRIP and backflow effects were characterised by inducing varying axial loads during the phase transformations. For all phase transformations, the observed TRIP and backflow strains varied in dependence of the load case. For the pearlite phase transformation, the axial loads led to a plastic deformation during the test which influenced the transformation behaviour. For lower stresses, the beginning of the phase transformation was delayed and the duration was extended due to the applied loads. As the time until pearlite is transformed and the duration of the transformation are relatively long, the effects are considered very low in the context of hot forming and therefore can be neglected. The bainite phase transformation did not show abrupt changes and also the microstructure showed shares of a different structure, hence it is unclear if the complete transformation was recorded. For the tested time interval for bainite, comparably low TRIP strains of 0.7 % for the compressive loading and 0.74 % for the tensile loading were measured and a much higher backflow strain of 0.56 % was observed for the tensile load than for the compressive load with 0.15 % and all other tested parameter configurations. The martensite transformation showed a higher TRIP strain of 1.55 % for the tensile load case than for the compressive case with 1.32 % whilst also showing the highest overall TRIP and backflow effects. As the most cooling routes of hot bulk forming process will result in a transformation of bainite and martensite, the results of this work emphasise the need of detailed material data to predict the transformation induced plasticity precisely by numerical simulation.

A more detailed investigation of the TRIP and backflow effects is planned to take lower axial loads, varying austenisation temperatures and longer holding times into consideration. The influence of the presumed carbide precipitations will be investigated through TRIP and backflow tests with an additional prior heat treatment. Also, the deformation dependent change of the TTT and CCT-diagrams will be characterised experimentally. With the extended experimental results, TRIP coefficients for a numerical simulation of a hot forming process will be derived for the steel 31CrMoV9.

## Acknowledgment

The authors thank the German Research Foundation (DFG) for the financial support of the project “Analysis of geometric deviations in long forged components, considering the influence of variable stress states on the transformation-induced plasticity” (Project number 511687873).

## References

- [1] T. Altan, G. Ngaile, G. Shen, Cold and hot forging. Fundamentals and applications, ASM International, Materials Park, OH, 2010.
- [2] M.C. Somani, L.P. Karjalainen, M. Eriksson, et al., Dimensional Changes and Microstructural Evolution in a B-bearing Steel in the Simulated Forming and Quenching Process, *ISIJ International* 41 (2001) 4, pp. 361–367.
- [3] B.-A. Behrens, A. Bouguecha, C. Bonk, et al., Numerical and experimental investigations of the anisotropic transformation strains during martensitic transformation in a low alloy Cr-Mo steel 42CrMo4, *Procedia Engineering* 207 (2017), pp. 1815–1820.
- [4] S. Denis, E. Gautier, A. Simon, et al., Stress–phase-transformation interactions – basic principles, modelling, and calculation of internal stresses, *Materials Science and Technology* 1 (1985) 10, pp. 805–814.
- [5] F.D. Fischer, G. Reisner, E. Werner, et al., A new view on transformation induced plasticity (TRIP), *International Journal of Plasticity* 16 (2000) 7–8, pp. 723–748.

- 
- [6] B.-A. Behrens, J. Uhe, H. Wester, et al., Experimental and numerical investigation of dynamic transformation induced plasticity during hot forming, *METAL* 2023, 2023, pp. 164–169.
- [7] F. Schweinshaupt, M. Müller, T. Herrig, et al., Thermoviscoplastic modeling of the shearing process for mechanism-driven fine blanking of high manganese steel, *Material Forming*, 2025, pp. 1856–1867.
- [8] J.H. Park, M.K. Razali, J.D. Yoo, et al., Modelling of hot flow behaviors of aluminum alloy Al6061 at elevated temperature: A review, *International Conference on Smart Materials and Structures (ICSMS-2022)*, Andhra Pradesh, India, 2023, paper 20005.
- [9] J. Němec, L. Kunčická, P. Opěla, et al., Determining Hot Deformation Behavior and Rheology Laws of Selected Austenitic Stainless Steels, *Metals* 13 (2023) 11, article 1902.
- [10] L. Taleb, N. Cavallo, F. Waeckel, Experimental analysis of transformation plasticity, *International Journal of Plasticity* 17 (2001) 1, pp. 1–20.
- [11] M.J. Holzweissig, D. Canadinc, H.J. Maier, In-situ characterization of transformation plasticity during an isothermal austenite-to-bainite phase transformation, *Materials Characterization* 65 (2012), pp. 100–108.
- [12] B.-A. Behrens, A. Bouguecha, C. Bonk, et al., Experimental investigations on the transformation-induced plasticity in a high tensile steel under varying thermo-mechanical loading, *Computer Methods in Materials Science* 17 (2017) 1, pp. 36–43.
- [13] M. Wolff, M. Böhm, M. Dalgic, et al., Parameter identification for a TRIP model with backstress, *Computational Materials Science* 37 (2006) 1–2, pp. 37–41.
- [14] B. Suhr, F. Frerichs, I. Hüßler, et al., Evaluation of models for martensitic transformation and TRIP via comparison of experiments and simulations, *Materialwissenschaft und Werkstofftechnik* 40 (2009) 5–6, pp. 460–465.
- [15] J. Trzaska, A. St. Jagiełło, L.A. Dobrzański, The calculation of CCT diagrams for engineering steels, *Archives of Materials Science and Engineering* 39 (2009), pp. 13–20.
- [16] M. Sommer, S. Hoja, M. Steinbacher, et al., Investigation of Compound Layer Structures after Nitriding and Nitrocarburizing of Quenched and Tempered Steels, *HTM Journal of Heat Treatment and Materials* 76 (2021) 3, pp. 219–236.
- [17] J.E. Hoffmann, M. Zgani, D. Scholz, et al., X-ray Residual Stress Analysis of Nitrided Low Alloyed Steels, *Materials Testing* 54 (2012) 6, pp. 395–407.
- [18] N. Fonstein, N. Pottore, S.H. Lalam, et al., Phase transformation behavior during continuous cooling and isothermal holding of aluminum and silicon bearing TRIP steels, *Proceedings of the Materials Science and Technology Conference*, 2003.
- [19] U. Ahrens, Beanspruchungsabhängiges Umwandlungsverhalten und Umwandlungsplastizität niedrig legierter Stähle mit unterschiedlich hohen Kohlenstoffgehalten, *Dissertation*, Universität Paderborn, 2003.
- [20] B.-A. Behrens, K. Brunotte, H. Wester, et al., Methodology to Investigate the Transformation Plasticity for Numerical Modelling of Hot Forging Processes, *Key Engineering Materials* 926 (2022), pp. 547–558.